4115

DRAFT
ROBERTSON ET AL

DESIGN AND ANALYSIS OF DEEP TWO-WELL TRACER TESTS

HYDROLOGY DOCUMENT NUMBER 612

by

John B. Robertson
Peter S. Huyakorn
Terry D. Wadsworth
and
John E. Buckley

HydroGeoLogic, Inc.
Herndon, Virginia

December 1987

Prepared for EWA, Inc., Minneapolis, Minnesota, in support of technical investigations for the Yakima Indian Nation

TABLE OF CONTENTS

LIST OF FIGURES

LIST OF FIGURES (continued)

LIST OF TABLES

Design and Analysis of Deep Two-Well Tracer Tests[1]

by John B. Robertson, Peter S. Huyakorn,
Terry D. Wadsworth, and John E. Buckley

ABSTRACT

Two-well tracer tests are among the few methods available for field measurement of effective porosity and longitudinal dispersivity in geologic formations. Injection-withdrawal tests, with and without recirculation, have used and proposed for characterizing hydrologic conditions at candidate repository sites for high-level nuclear waste, such as a portion of the U.S. Department of Energy's Hanford Reservation in the State of Washington. Target formation depths can typically be greater than 3000 feet. At these depths the transport time of the tracer in the well-bore conduits may be much greater than through the tested formation.

Traditional methods for interpreting two-well tracer tests have been based on simplified analytical models which ignore potentially important effects such as vertical layering, heterogeneity, matrix diffusion, variable flow rates, recirculation of tracer, and transport through piping. To overcome these and other limitations a new, finite-element numerical code has been developed, STACE3D, (Seepage and Transport Analysis using Curvilinear Elements in 3 Dimensions).

[1] Work done for EWA, Inc. in support of their contract with the Yakima Indian Nation

The code is specifically designed to analyze subsurface transport problems in which the flow field is curvilinear, such as that associated with a pumping and injection well couplet. Another unique feature of the code is a component which simulates flow and Taylor's dispersion in the well-bore conduits. This feature allows, for the first time, consideration of variations in pumping rates and recirculation of tracer through the entire system. The composite code was used to analyze two two-well tracer tests previously conducted in a deep basalt formation at the Hanford Reservation, Washington (Wells DC-7 and DC-8). The results demonstrate the capabilities of the code and confirm that Taylor's dispersion under laminar flow in piping can be at least as important as dispersion in the formation.

A close match of simulated results to field results was obtained for both the first and second recirculated tracer breakthrough peaks for field test #2. Apparent effective porosity for that test is 1.0×10^{-4} and apparent formulation longitudinal dispersivity is 0.8 ft based on the new, more comprehensive analysis. If simplified analytical methods are used, order of magnitude errors in apparent effective porosity can result from relatively small errors in flow rates or well-bore conduit volume. It is therefore important that careful attention be paid to accurate flow rate and bore-hole conduit volume measurement in the design and implementation of deep-well test.

1. INTRODUCTION

Many hydrogeologic studies are aimed at characterizing and evaluating potential waste disposal sites, assessing known or suspected groundwater contamination problems, and other objectives requiring knowledge of solute transport properties of the geologic media. Among the specific parameters needed for assessing solute transport properties are effective porosity (n_e), longitudinal dispersivity (α_L), sorption distribution coefficients (K_d), and perhaps matrix diffusion characteristics of the rock mass. A specific example of these requirements is in the high-level nuclear waste repository program of the United States. One of the regulatory requirements of that program is that groundwater travel time from the repository to the border of the controlled area around the repository be greater than 1000 years. Demonstrating compliance with this requirement requires an accurate assessment of groundwater velocities which, in turn, requires accurate and representative measurements of effective porosities (among other parameters). Another requirement in the nuclear waste program, as well as other environmental regulations, is that concentrations of radionuclides or other hazardous substances in groundwater migrating away from regulated facilities be lower than specified maximum limits. Again, demonstrating compliance to concentration limits requires measurements of dispersivities and other solute transport properties of the geologic formations involved.

One of the few available field methods for determining effective porosity and longitudinal dispersivity is the two-well injection-withdrawal tracer test. In this type of test, a suspended or dissolved tracer (chemical, radionuclide, or suspended microparticles) is injected into a well in which water is continually injected; the arrival or "breakthrough" concentration profile is observed in a nearby well which is being pumped. The shape of the plot of concentration versus time for the withdrawal well is then fitted to type curves from an analytical or numerical model to determine effective porosity and longitudinal dispersivity. In a case where the water pumped from the withdrawal well is recirculated as the injection water for the injection well, the test is called a recirculating two-well tracer test.

Several methods have been developed and applied to analyze two-well tracer tests, with and without recirculation (Grove and Beetem, 1971; Webster and others, 1970; Gelhar, 1982; Lenda and Zuber, 1970; Zuber, 1974; and Pickens and Grisak, 1981). These methods are based on simplified analytical solution models and thus have some rather severe limitations and constraints. Among the assumptions or requirements that must be satisfied to apply these methods are:

- the tested formation is a single layer with uniform homogeneous and isotropic properties

- injection and withdrawal rates are equal and constant with time (Gelhar's method allows for unequal rates but they must remain constant)
- effects of tracer transport through the boreholes and piping is negligible
- lateral dispersion effects are insignificant.

Many real-world test conditions deviate significantly from these requirements and therefore might be subject to unacceptable errors by applying the available analytical solution methods. Recent developments in numerical methods have expanded analytical capabilities to include condition of multiple formation layers, heterogeneity and anisotropy, and varying pumping and injection rates (Huyakorn and others, 1986a, 1986b).

Despite these developments, a particular concern remained for deep two-well tracer tests; that is, those tests in which the wells are deep enough or large enough that travel time of the tracer in the wells and piping approaches or exceeds the travel time through the formation along the direct pathway connecting the wells. In nuclear waste repository investigations, for instance, typical target depths are 1000 to 4000 feet. If a two-well tracer test is conducted at a depth of 3000 feet, travel time of the tracer in the well-bores and piping can easily be a factor of ten or more than travel time in the formation. In that case, an error of ten percent in calculated travel time in the piping can translate to calculated effective

porosity errors on the order of a factor of 2, 3, or even more. Furthermore, if the plumbing system has a large volume relative to the formation, Taylor's dispersion phenomena in the well-bore piping might cause significant dispersion effects which could be erroneously attributed to the dispersivity of the formation.

In recirculating tests where the tracer is introduced as discrete slug, there has been no way to account for or analyze the recirculated second or third breakthrough concentration peaks that occur when the first peak is recirculated back through the injection-withdrawal system. This is because formerly available models had no transport component for travel time through the wellbores and piping.

2. OBJECTIVES

The objectives of this study were two-fold:

1. Develop a numerical model which could accurately analyze two-well tracer tests including the following processes and characteristics:
   a. variable pumping and injection rates
   b. stratified formation flow
   c. transport phenomena, including Taylor's dispersion through the well bores and piping
   d. recirculation of the original and secondary tracer peaks

e. matrix diffusion, adsorption, and radioactive decay of the tracer.

2. Demonstrate the model on actual field tests conducted in deep basalt formations at the candidate nuclear repository site on the U.S. Department of Energy's Hanford Reservation in the State of Washington.

Although the primary objective was to develop a more reliable and accurate method of analyzing complex deep-well tracer tests, a secondary objective included an assessment of the relative importance or significance of Taylor's dispersion phenomena in lengthy planning systems of such tests.

3. TECHNICAL APPROACH

The approach selected for this study was to develop a modular numerical model with components and options capable of addressing significant aspects of the test. The major components are shown in Figure 3.1 and include the geologic formation, the injection well, and the withdrawal well.

3.1 Flow and Transport in the Geologic Formation

The formation flow and transport model has the flexibility for handling groundwater flow and solute transport, or either of these processes separately. The finite element flow model component assumes flow of the fluid phase is isothermal and governed by Darcy's Law (Huyakorn and Pinder, 1983) and that the fluid considered is slightly compressible and homogeneous. The transport model component assumes isotropic porous media,

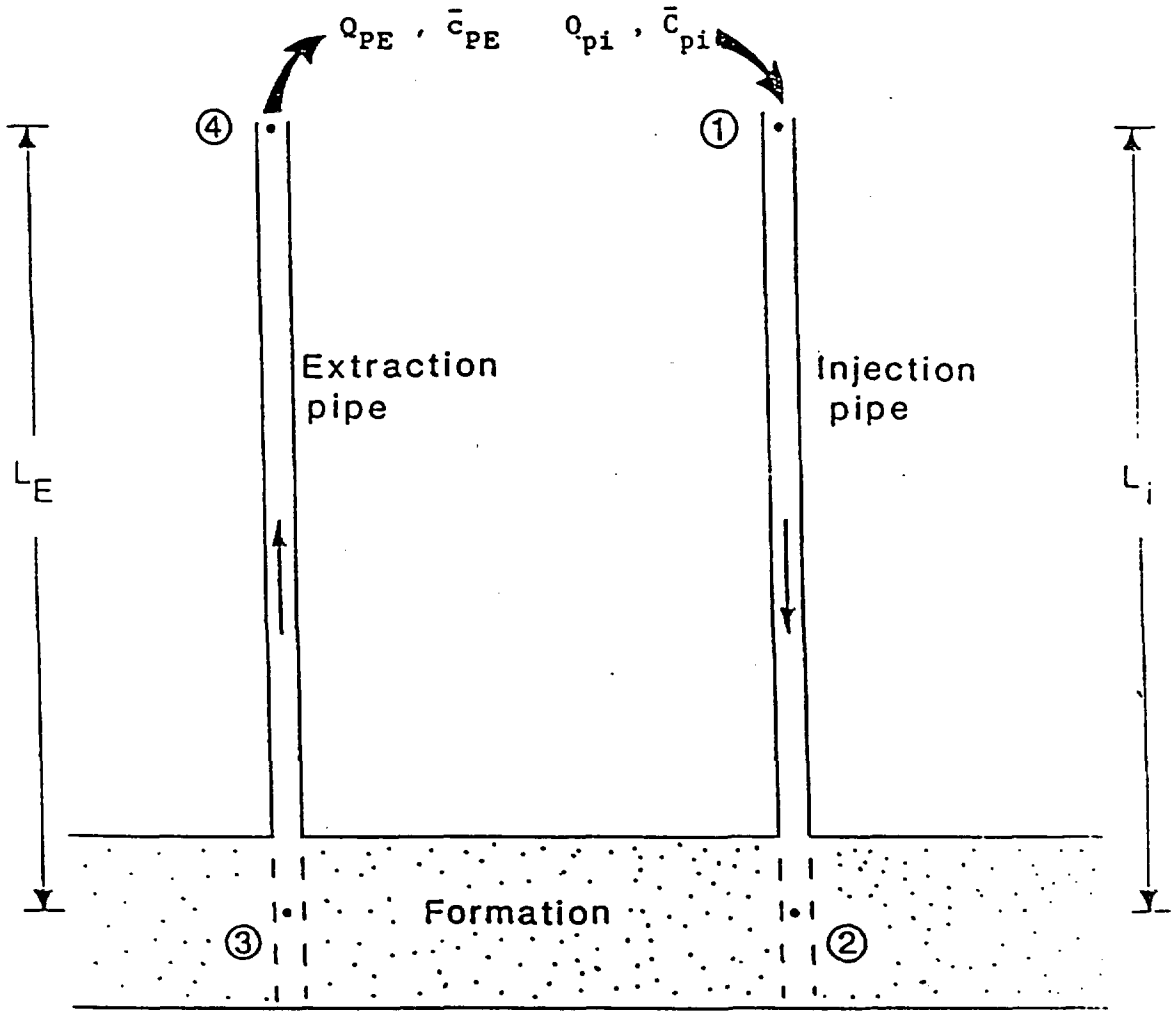

Figure 3.1. Schematic diagram illustrating three main components of STACE3D model for deep two-well tracer tests (injection pipe, extraction pipe, and geologic formation) and four component interfaces (labeled 1, 2, 3, and 4). L is pipe length, Q is flow rate, and c is average tracer concentration.

linear equilibrium adsorption, and that transport is governed by Fick's Law (Freeze and Cherry, 1979). Hydrodynamic dispersion, equilibrium sorption, first-order decay, and molecular diffusion are included in the transport processes.

The model performs three-dimensional, two-dimensional, or axisymmetric finite element solutions to the flow and transport equations for confined aquifer systems. The conventional Galerkin finite element technique formulated in rectangular or curvilinear coordinates (Huyakorn and others, 1986a) is used to solve the groundwater flow equation. Several implicit schemes are available to solve the convective-dispersive transport equation also formulated in rectangular or curvilinear coordinates. For a detailed description of the solute procedures, the reader is referred to the code documentation (Huyakorn and others, 1987).

The model is especially designed to perform the analysis of double well tracer tests in stratified aquifers but it can also simulate a wide range of saturated groundwater problems. The code (STACE3D) can also be used to predict the response of a groundwater basin to different well pumping operations, predict the extent of contaminant plumes and rate of plume migration, aid in the design of groundwater quality monitoring programs, and perform risk analysis from a waste site.

The code is written in FORTRAN 77 and no computer dependent features have been included. All arrays have been stored in main core memory and hence no backup peripheral devices are

needed during code execution. The code is currently operational on a mini or mainframe computer and requires 188 K bytes of storage.

3.2 Flow and Transport in Piping

Dispersion and transport time may have an important or even predominant role in deep two-well tracer tests. Therefore, it is desirable to incorporate these components of the flow system into the simulation code. Transport through well-bore linings and other piping or conduits can be described by the following one-dimensional equation:

$$\bar{D}_p \frac{\partial^2 \bar{c}_p}{\partial z^2} - \bar{v}_p \frac{\partial \bar{c}_p}{\partial z} = \frac{\partial \bar{c}_p}{\partial t} \qquad (3.1)$$

where z is the local coordinate along the length of each pipe, $\bar{c}_p$ and $\bar{v}_p$ are average values of concentration and velocity over the cross section of the pipe, $\bar{D}_p$ is the cross-section averaged dispersion coefficient, and t is elapsed time.

Flow in pipes may be laminar or turbulent depending on the magnitude of Reynolds number, R_e. For laminar flow ($R_e \leq 2000$), the dispersion coefficient, $\bar{D}_p$ can be calculated from Taylor's formula (Taylor, 1953; Chatwin, 1970). For turbulent conditions ($R_e \geq 20000$), $\bar{D}_p$ is much smaller and can be calculated with a different method (Nunge and Gill, 1970; Dullien, 1979). A more detailed discussion of $\bar{D}_p$ calculation can be found in Huyakorn and others (1987).

The solution of equation (3.1) first requires the establishment of boundary conditions, including an interface boundary condition where the well bores and formation are linked.

The numerical approximation of equation (3.1) uses the upstream weighted residual technique and one-dimensional linear finite elements. A standard Crank-Nicholson central difference scheme is used for time stepping. Additional details of the boundary conditions and solution algorithms used can be found in Huyakorn and others (1987).

Input data required for the pipe-transport components of STACE3D are:

- Pipe geometry -- radius and length
- Flow rate data -- pipe flow rate versus time
- Properties of water -- kinematic viscosity
- Dispersion coefficient for tracer, $\bar{D}_p$
- boundary and initial conditions including tracer input data

3.3 Composite Formation and Pipe-Flow Model

A diagrammatic sketch of the composite transport model including formation and piping components for the two-well tracer test system is illustrated in Figure 3.1. Common interface boundaries correspond to the four junctures labeled 1, 2, 3, and 4. The pipe and formation flow and transport components are linked numerically in the integrated composite code which is used for the applications discussed in this report.

3.4 Verification of Geologic Component and Examples

3.4.1 Comparison with Two Analytical Solutions

To further verify the accuracy of the geologic formation component of the STACE3D code, a sample problem was set up which could also be solved by established analytical models. The sample problem is similar to field test conditions for an actual test conducted at the U.S. Department of Energy's candidate site for a high-level nuclear waste repository on the Hanford Reservation, Washington (Tracer Test 1). Details of the tracer test site conditions are described in a later section of this report.

The sample problem has the following assumed conditions:

- pumping and injection rates are equal and constant at 2.8 gpm
- tracer is injected as a discrete short-time pulse
- well spacing is 46 ft
- longitudinal dispersivity is 3.2 ft (no lateral dispersivity)
- no recirculation of tracer
- no sorption or matrix diffusion effects
- geologic formation is of uniform thickness, is homogeneous and isotropic; flow is two dimensional and horizontal.

The analytical methods selected are the Gelhar (1982) method and the method of Hoopes and Harleman (1967). Hoopes and Harleman's method has been validated with laboratory

experiments and is widely accepted. Gelhar's method represents some improvements and was previously used for analyzing the Hanford site field tests, as described in the next section.

Simulation results from the two analytical models and the STACE3D numerical code (without pipe-flow components) are depicted in Figure 3.2. It is apparent that the Gelhar and Hoopes and Harleman analytical methods yield similar results, with Gelhar's method predicting a steeper, less dispersed arrival phase of the peak. The early differences between Gelhar's and Hoopes and Harleman's methods are probably a result of the additional terms in the analytical solution equation which Gelhar considers, thereby eliminating some erroneous mathematical dispersion.

The numerical peak has an even steeper arrival than Gelhar's, due to the more complete and accurate solution of the governing equations. The slight differences in peak height and arrival time are also attributable to the fewer simplifying assumptions inherent in the numerical finite element approach. The results of this test confirm that the STACE3D numerical code yields results comparable to the analytical methods but with less mathematical or numerical dispersion. The STACE3D code has previously been successfully tested against other example problems also (Huyakorn and others, 1986b, 1987).

To demonstrate the sensitivity of the test problem model to the formation longitudinal dispersivity, three simulations were conducted with STACE3D using different longitudinal

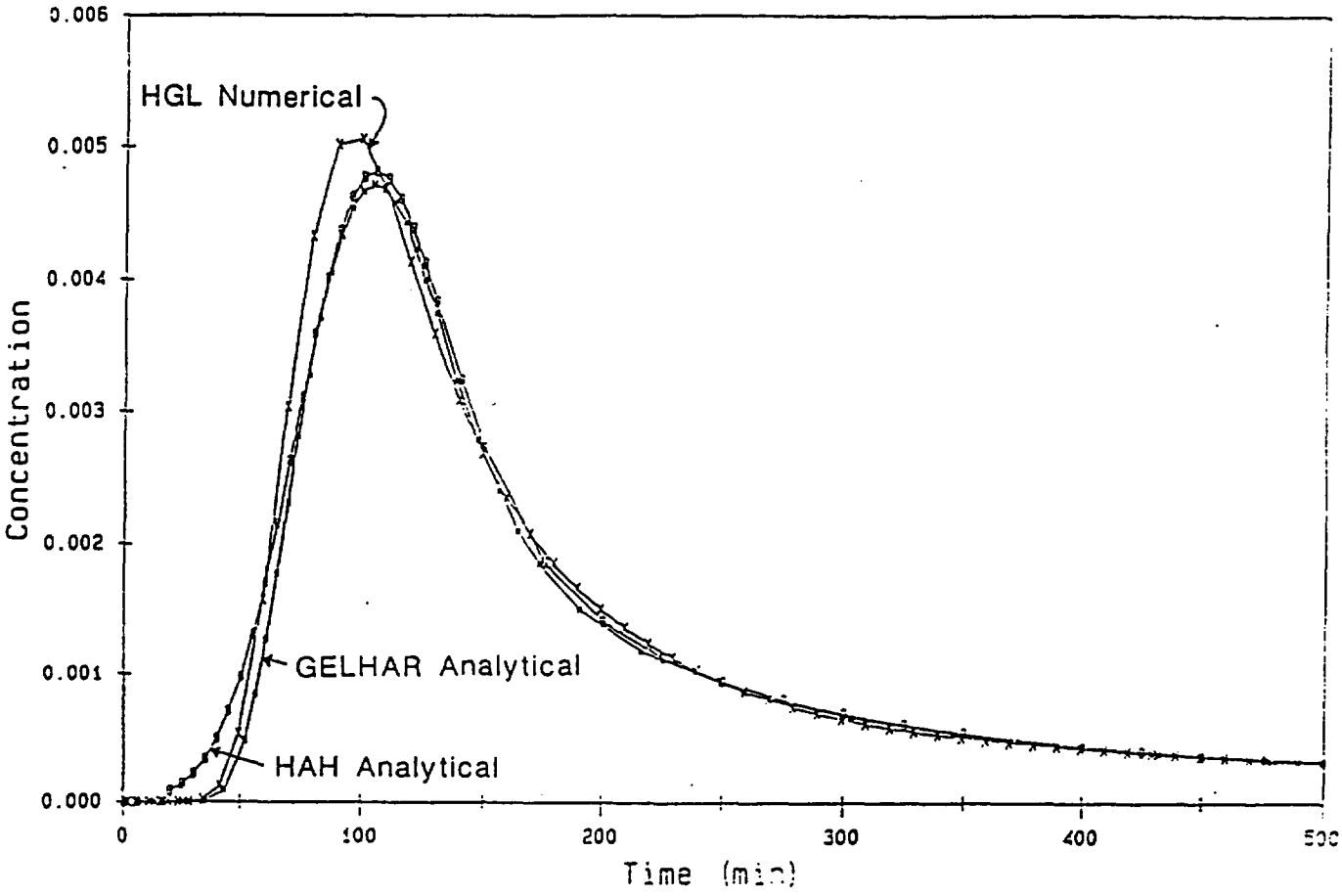

Figure 3.2. Comparison of HydroGeoLogic's (HGL) numerical solution using STACE3D code (without pipe flow components) to analytical solutions of Gelhar (1982) and Hoopes and Harleman (1967), HAH, for sample problem described in text.

dispersivities. The results are shown on Figure 3.3. It is apparent that increasing the dispersivity causes the expected effects of spreading the early arrival phase of the peak and shifting the magnitude and location of the peak maximum.

4. ANALYSES OF HANFORD FIELD TESTS

4.1 Description of Test Conditions

As part of the site investigations for a potential high-level nuclear waste repository location at the DOE Hanford site in the State of Washington, two tracer tests were conducted in 1979 and 1981 using the two-well tracer pulse technique in a deep basalt flow-top formation (Wells DC-7 and DC-8). The basic physical characteristics of the tests are described by Gelhar (1982) and Leonhart and others (1982) and are summarized in Figure 4.1a. Important features of each test are summarized as follows:

	TRACER USED	PUMPING RATE	WELL DEPTH	DISTANCE BETWEEN WELLS	OTHER COMMENTS
TEST 1:	radioactive I-131	variable 1 to 8 gpm	3415 ft	46 ft	pumping and injection rates were variable and unequal for portions of test
TEST 2:	potassium thiocyanate	steady at about 1 gpm	3415 ft	46 ft	full recirculation throughout test

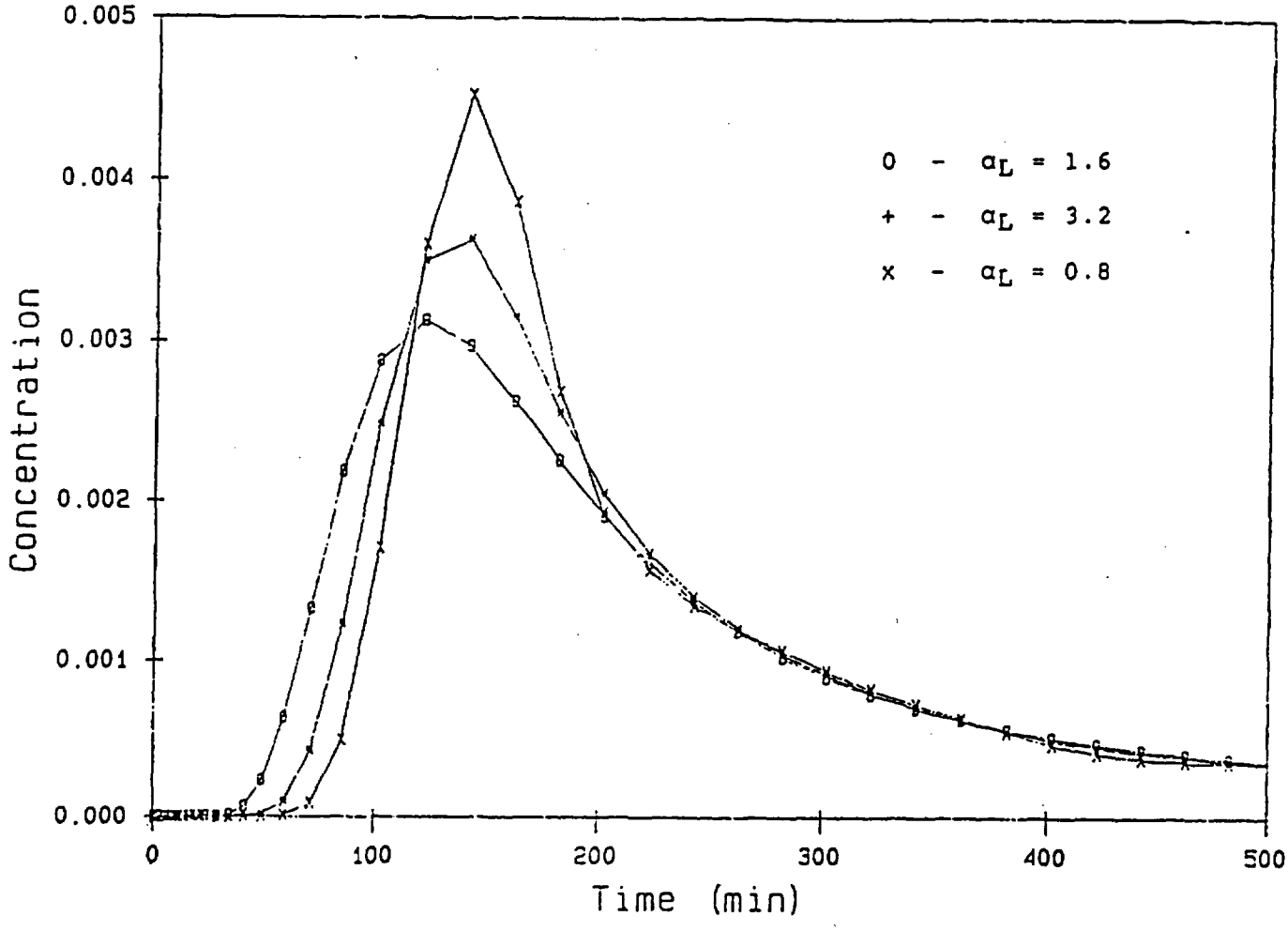

Figure 3.3. Effects of varying longitudinal dispersivity (a_L) of the geologic formation using STACE3D model without pipe-flow components. The sample problem is the same as that for Figure 3.2.

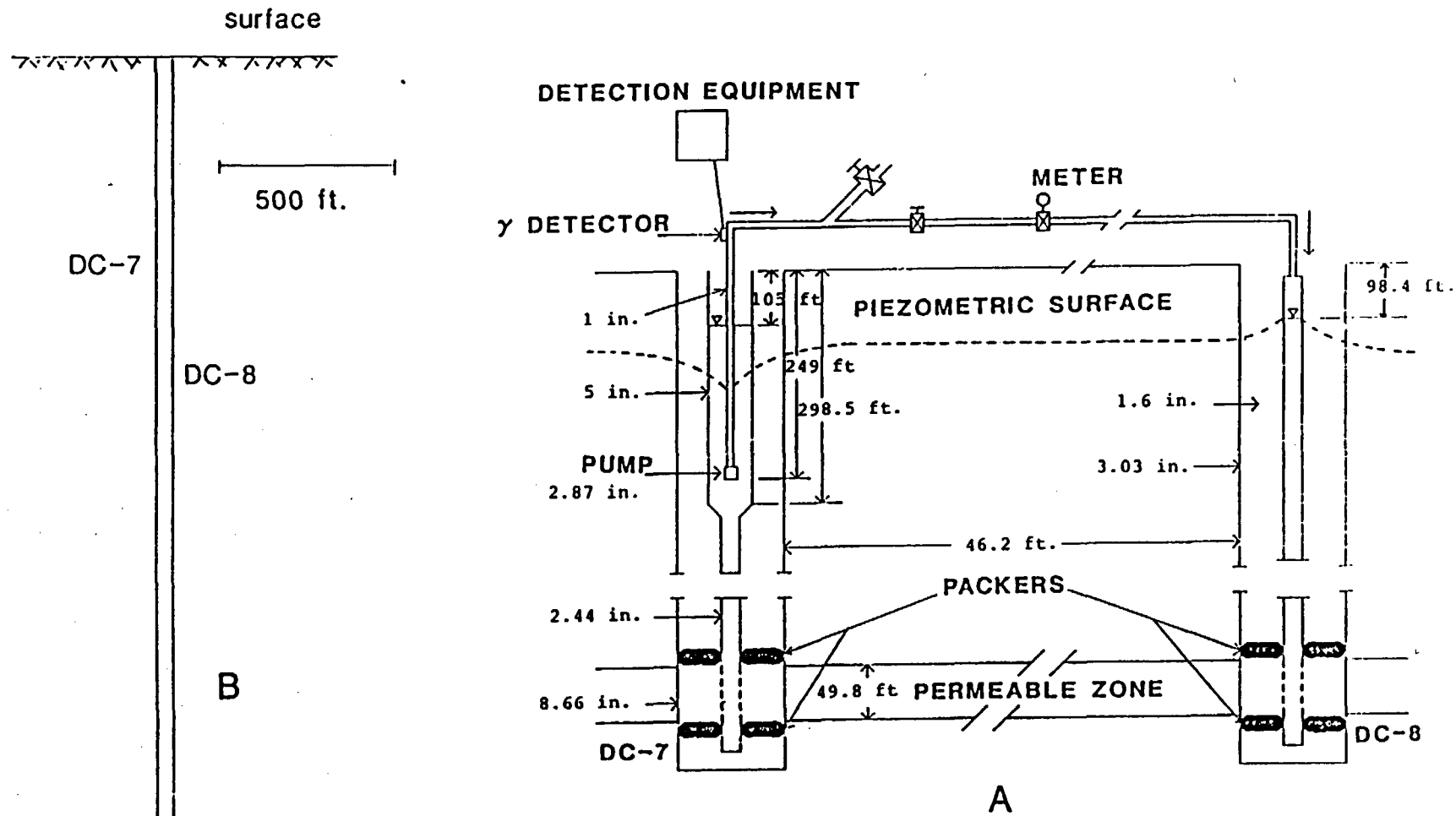

Figure 4.1. A: Diagram of DC-7, DC-8 two-well tracer test field conditions, Hanford site, Washington, showing well piping system and other key features, with exaggerated horizontal scale (total depth of wells is 3415 feet).
B: DC-7, DC-8 test conditions drawn to true scale to emphasize length of wells compared to horizontal separation.

For proper perspective, Figure 4.1b shows the test geometry at true scale, indicating the long travel distance through the wells compared to the formation length between the wells.

The most significant complication in Test 1 is that withdrawal and injection rates varied and were unequal during much of the test. There is also some ambiguity in the pumping and injection rates reported for the test (Gelhar, 1982).

In order to use any of the analytical models, the travel times of the tracer down the injection well and up the pumping well must be precisely determined, so that they can be subtracted from the actual total travel times observed at the surface tracer detection system. It is apparent that changes in pumping or injection rates during the test greatly complicate calculations of tracer travel time up and down the wells. Also, a change in pumping rate can significantly alter the shape of the tracer breakthrough curve and can lead to erroneous estimates of effective porosity and dispersivity. For this reason, Test 1 is much more subject to error using the simplified analytical methods than is Test 2. Both tests were originally analyzed using the Gelhar method, as reported by Gelhar (1982) for Test 1 and by Leonhart and others (1982) for Test 2. In the following sections, their results will be compared to ours, using the more comprehensive numerical model STACE3D with and without pipe-flow components.

4.2 Test 2 Simulations

Simulation results for Test 2 will be presented first because that test was more carefully controlled and had fewer complications.

4.2.1 Composite STACE3D Model

After completing development and testing of the numerical code for flow and transport in the well-bore piping (including Taylor's dispersion), the pipe-flow code was coupled to the original STACE3D code which simulates flow and transport through the formation. The composite code was then applied to simulate Test 2 conditions. The unknowns which were varied are effective porosity of the formation and longitudinal dispersivity of the formation and the piping. Pipe dispersivity (for Taylor's dispersion) depends mostly on pipe geometry and roughness, fluid velocity, and the molecular diffusion coefficient of the tracer. For turbulent flow at high velocities, pipe-flow dispersion is low; for laminar flow in pipes, dispersion can be relatively high. Initial estimates of Taylor's dispersion coefficients were assigned based on known pipe and discharge characteristics.

After several trial and error curve fitting adjustments, a close match was obtained between simulated results and field data (Figure 4.2). The recirculated second tracer peak clearly appears at the proper position and magnitude. This simulation represents the first time (to our knowledge) that a fully recirculating tracer test in a deep formation has been success-

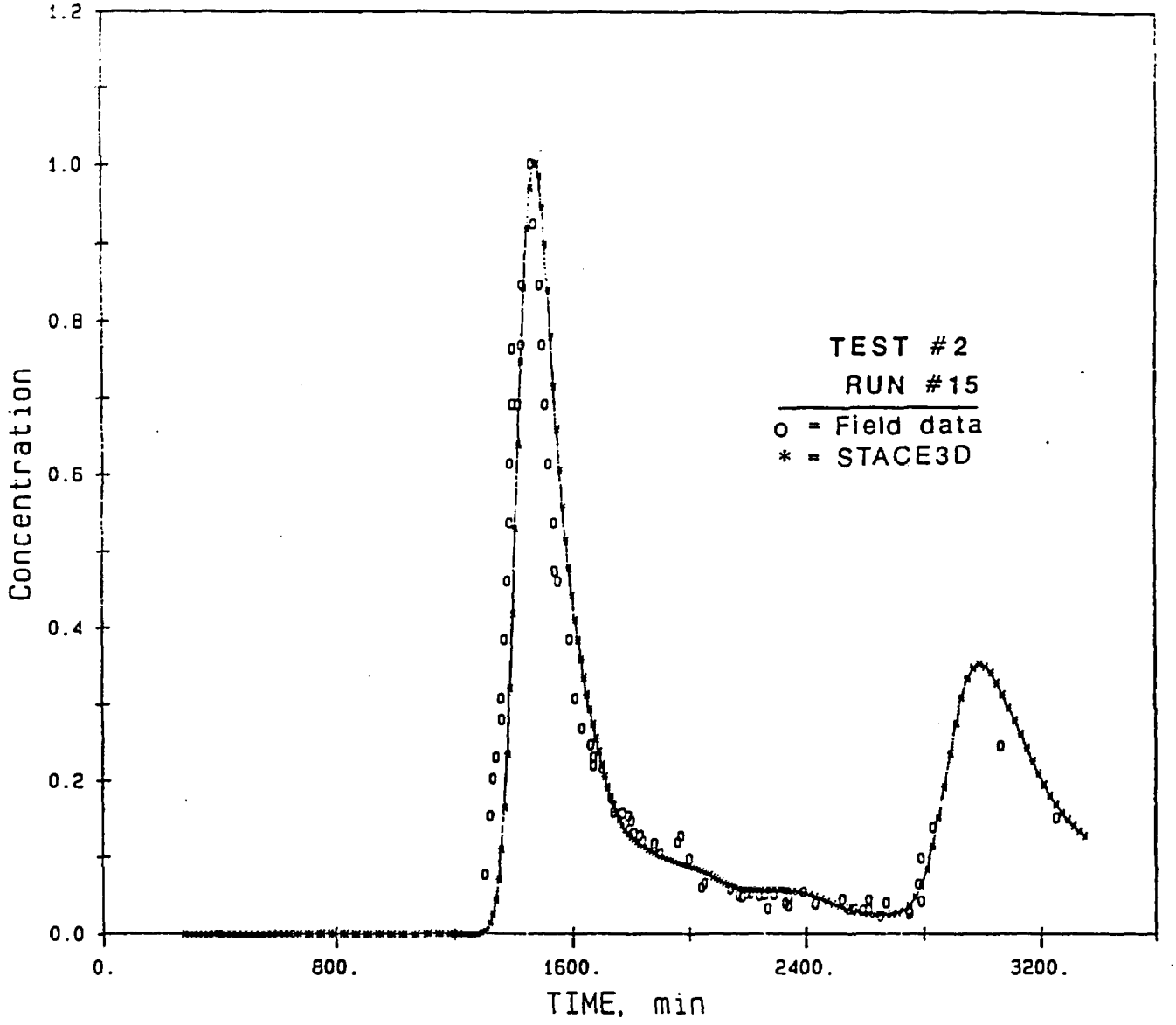

Figure 4.2. Comparison of best-fit simulation run from composite STACE3D model to field data from Hanford Tracer Test 2, indicating correct prediction of first arrival peak and secondary recirculation peak.

fully simulated, including secondary peaks. The parameters associated with this best-fit case are:

Effective porosity, n_e	=	1×10^{-4}
Longitudinal dispersivities		
Formation, α_L	=	0.8 ft
Injection well pipe, α_{Lpi}	=	10 ft
Pumping well pipe, α_{Lpw}	=	2 ft
Flow rate, Q	=	0.88 gpm

In trying to obtain a good curve match, it became obvious that the reported flow rate, "about 1 gpm," for the test was slightly too high. We could not obtain a good fit until the simulated flow rate was lowered to 0.88 gpm. This discrepancy could be due simply to reasonable degree of error in the measured flow rate or to error in the total injection and pumping well piping volume (errors in reported pipe diameter or length).

A test of this type is extremely sensitive to error in either piping volume or flow rate, as shown on Figure 4.3, which compares simulation curves for 1 gpm and 0.88 gpm. The travel time of the tracer peak through the formation is only about 150 minutes compared to a travel time of about 1500 minutes through the total injection and withdrawal system. Therefore, any error made in calculating or measuring the travel time through the piping system translates to an error in

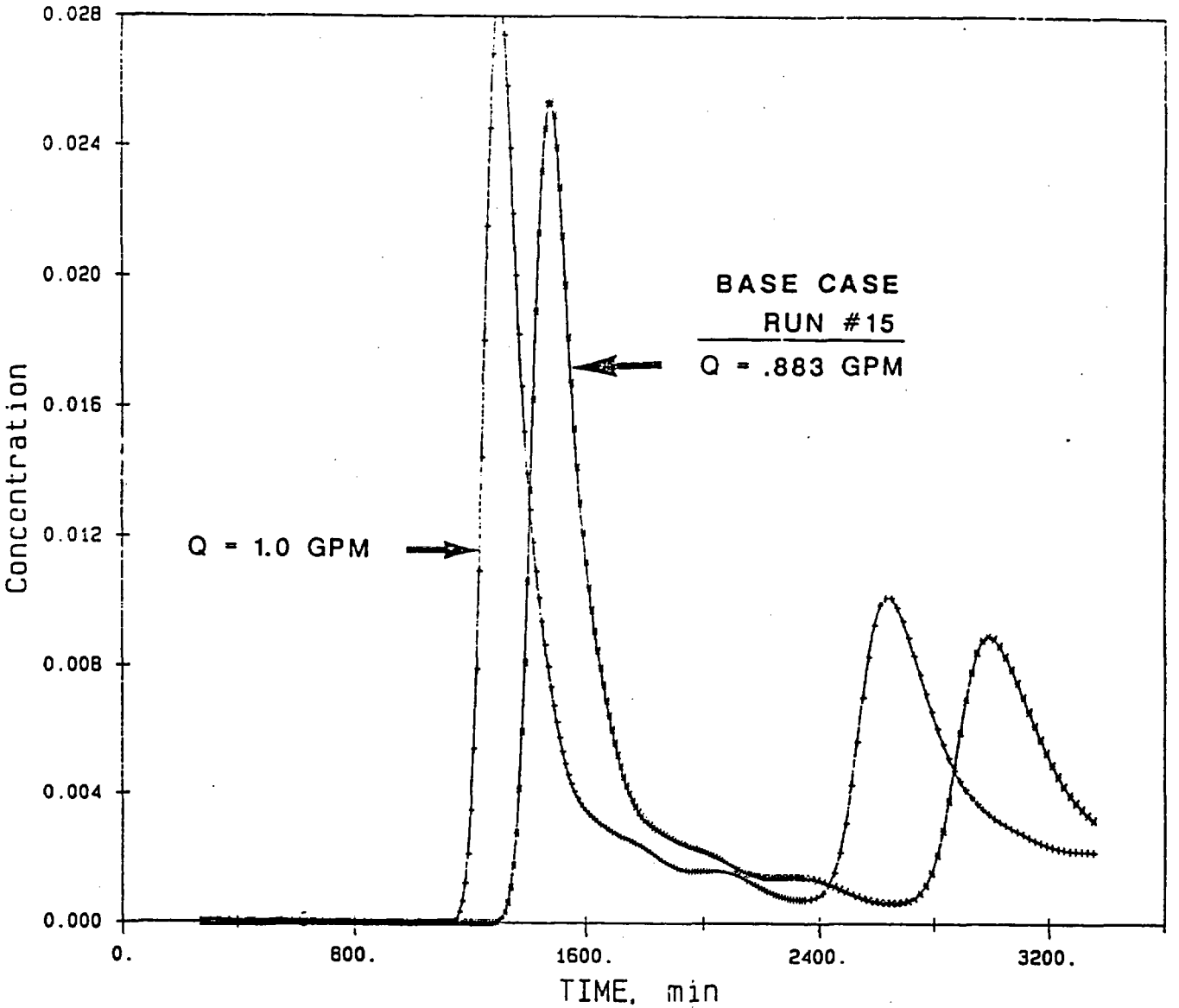

Figure 4.3. Effect of a 12-percent change in flow rates (injection and pumping) on tracer breakthrough curves simulated by STACE3D for Hanford Tracer Test 2.

formation travel time that is magnified by a factor of about 9, which, in turn, can cause an error of similar or greater magnitude in apparent effective porosity. Therefore, a 12 percent error in flow-rate (or piping volume) causes an error of about 60 minutes in the piping travel time, which is similar to the travel time through the formation. In that case, the calculated effective porosity could be several orders of magnitude too low (or even negative), if the piping flow time was erroneously high, or it could be a factor of about two too high, if the piping flow time underestimated by 12 percent.

Simulations of Test 2 also indicated that test results are sensitive to Taylor's dispersion in the piping. Figure 4.4 shows two simulations with different piping dispersivities. Test 2 conditions suggested laminar flow and corresponding piping dispersivities which were originally estimated to be in the range of 600 to 700 ft using standard formulas (Taylor, 1953; Chatwin, 1970). It became immediately apparent that the actual pipe dispersivities were much lower than originally estimated. The reasons for this may be roughness of the pipes or other phenomena not presently understood. The important point is that it is possible in these types of tests for Taylor's dispersion in the pipes to have a greater effect than dispersion in the formation. Furthermore, it is not possible to separate the effects of Taylor's dispersion from formational dispersion in the observed field data curve, unless Taylor's dispersion in the piping can be measured or reliably calculated independently.

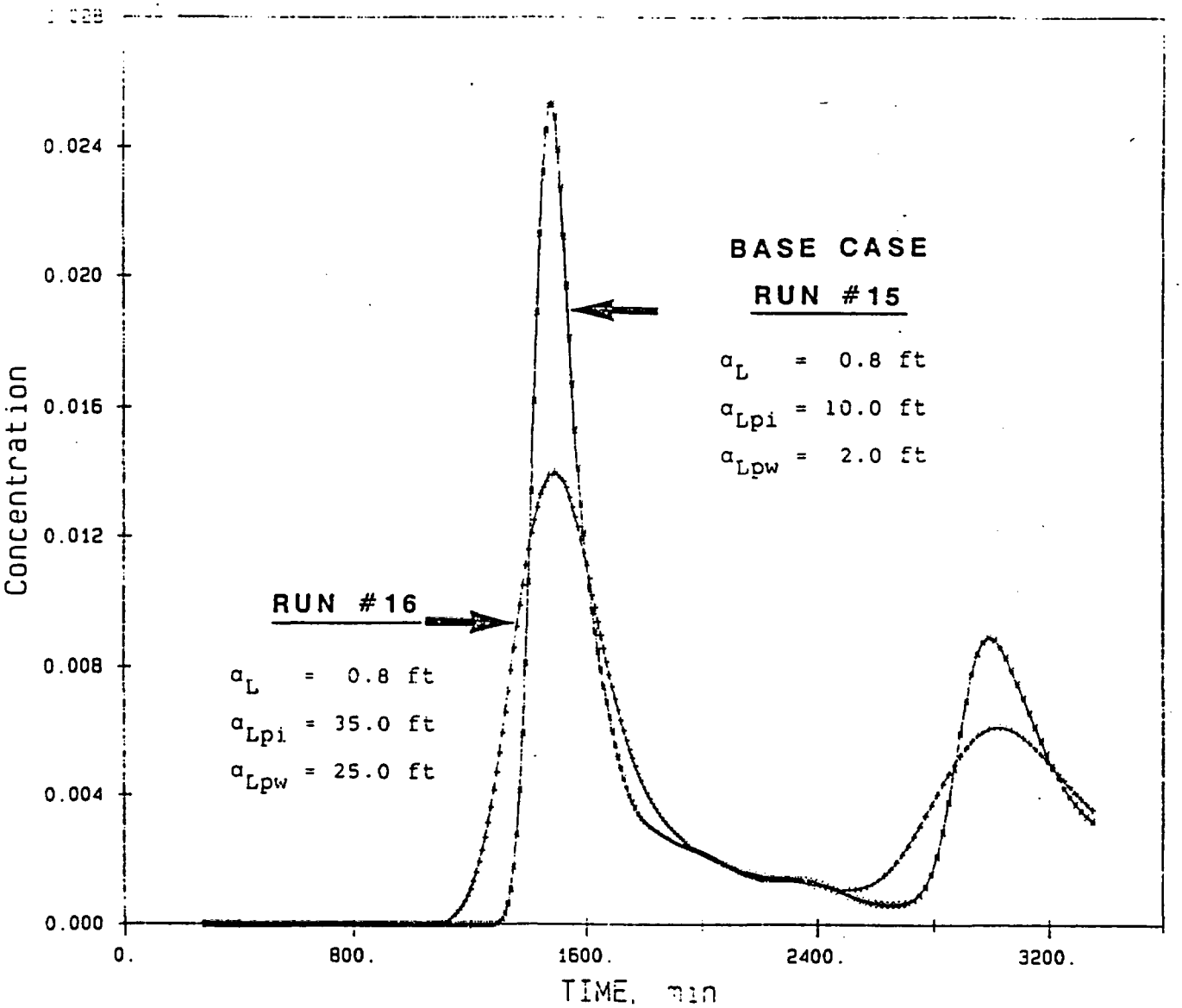

Figure 4.4. Effects of changes in piping dispersivities on tracer breakthrough curves simulated using STACE3D for Hanford Tracer Test 2. (α_{Lpi}, injection pipe; α_{Lpw}, pumping well pipe; α_L, formation longitudinal dispersivity).

One of the features of the STACE3D composite model is its capability to provide tracer breakthrough curves for any of four points of interest in the system, top and bottom of the injection well and top and bottom of the extraction well (Figure 3.1). The best-fit breakthrough curve shown in Figure 4.2 is for position 4, top of the extraction well. Corresponding curves for the other three positions in the model (together with position 4) are shown in Figures 4.5-a,b,c, and d. The effects of travel time, pipe dispersion, and formation dispersion can be seen as the peak traverses the circuit.

4.2.2 Simulations Without Pipe-Flow Components

Before incorporating the pipe-flow components of the composite model, Test 2 was simulated using only the formation flow and transport portion of STACE3D. Piping volume originally reported by SAI, Inc. (Gelhar, 1982) was used to estimate piping travel time. Our best fit for those simulations is shown in Figure 4.6. The apparent formational effective porosity is 1.5×10^{-4} and the longitudinal dispersivity is 1.5 ft. Because of the potential degree of error in piping travel time, it is perhaps fortuitous that the apparent effective porosity obtained from this simulation is similar to that obtained from the more comprehensive simulation discussed above. However, it is significant that the apparent dispersivity is nearly a factor of two higher than obtained from the composite model. We conclude that α_L is overestimated from the results in Figure 4.6 because the field curve includes the combined

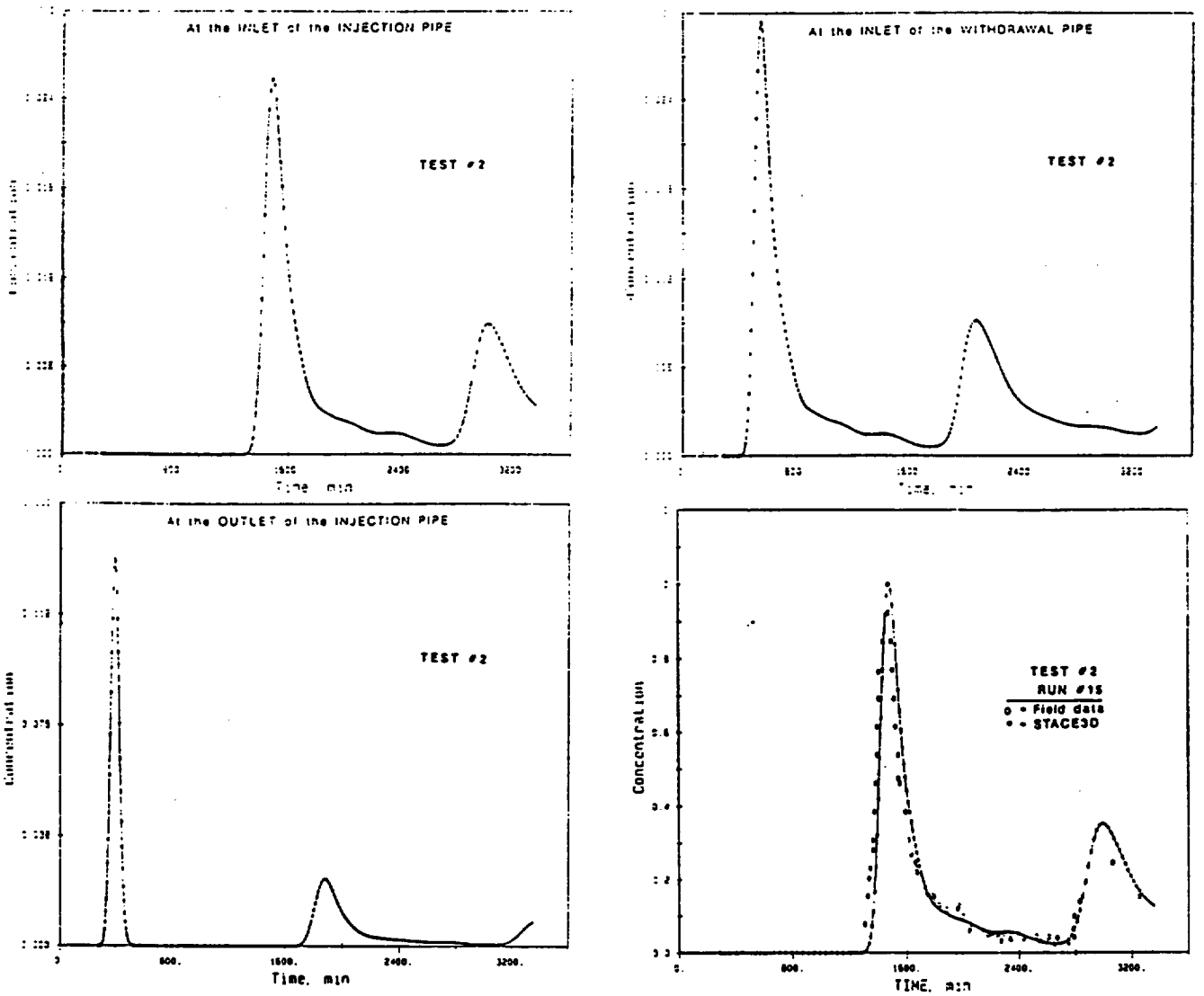

Figure 4.5. Tracer breakthrough curves for 4 positions of STACE3D composite model (see Figure 3.1) for Hanford Test 2 (concentrations are dimensionless).

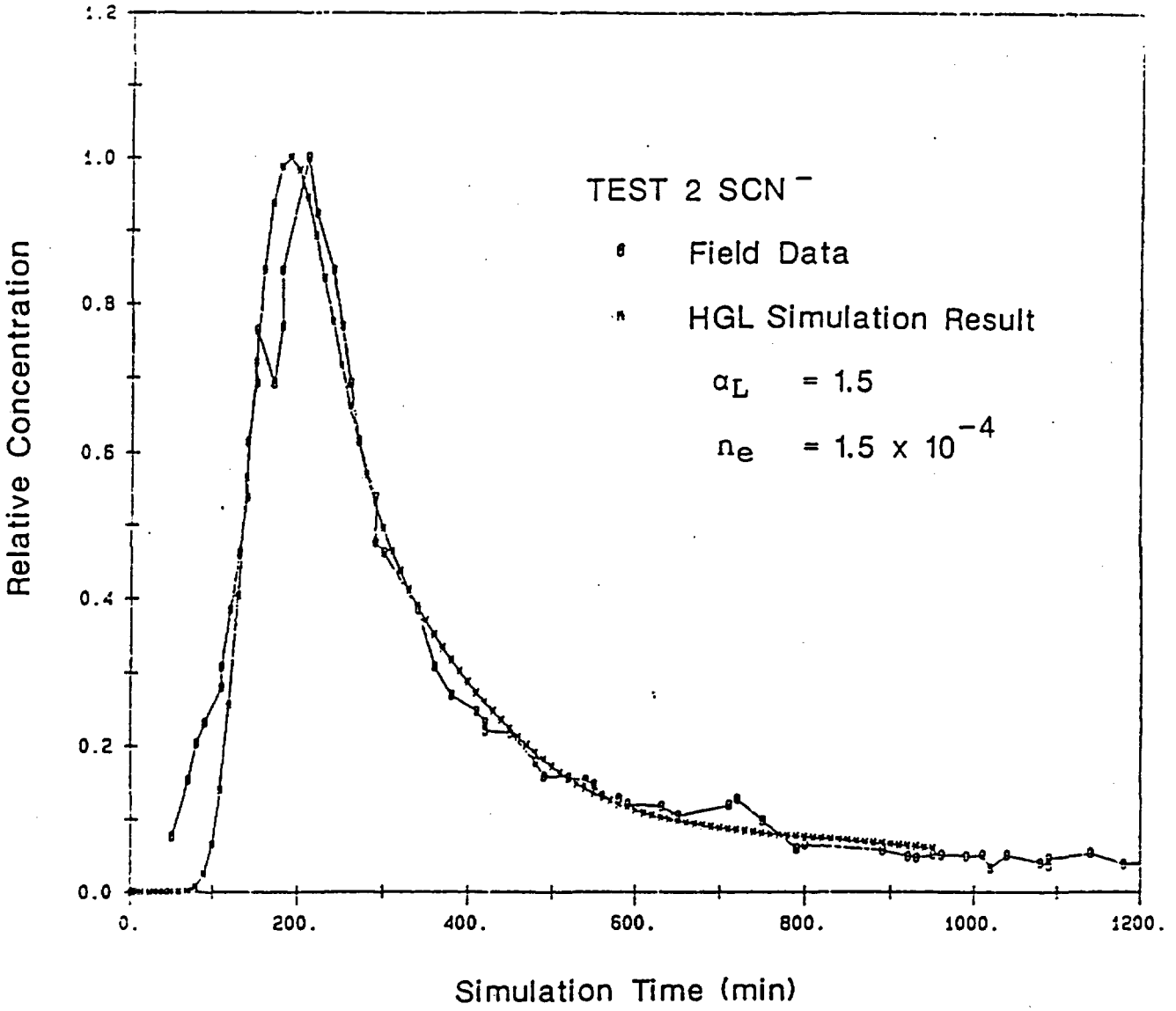

Figure 4.6. Comparison of STACE3D simulation (without pipe-flow component) with field data for Hanford Test 2.

effects of Taylor's dispersion and formation dispersion which cannot be separated in this simulation. This result further confirms the importance of considering Taylor's dispersion in deep-well tests.

4.3 Test 1 Simulations

As stated above, Test 1 had more complications and uncertainties, associated with variable pumping rates and unequal pumping, than did Test 2. This is illustrated in Figure 4.7 which shows pumping and injection rates during the test as reported by Gelhar (1982). During the most crucial part of the test, when the tracer peak was traveling through the formation (200 to 400 minute range), the injection and withdrawal rates were unequal. After the tracer peak had entered and was traveling up the withdrawal well, the pumping rate was significantly increased (at about 500 minute).

Gelhar (1982) originally analyzed the test using an analytical model capable of incorporating the effects of unequal injection and withdrawal rates. We performed a sensitivity analysis with Gelhar's method to evaluate the degree of error that might occur if the injection and withdrawal rates were assumed to be the same and equal to the mean of the actual rates. The results indicate that for Test 1 conditions, there is less than 5 percent error associated with assuming the flow rates are equal. Therefore, we felt justified in simplifying the simulations by assuming that the injection and withdrawal rates were equal at 2.8 gpm (the mean of the average injection

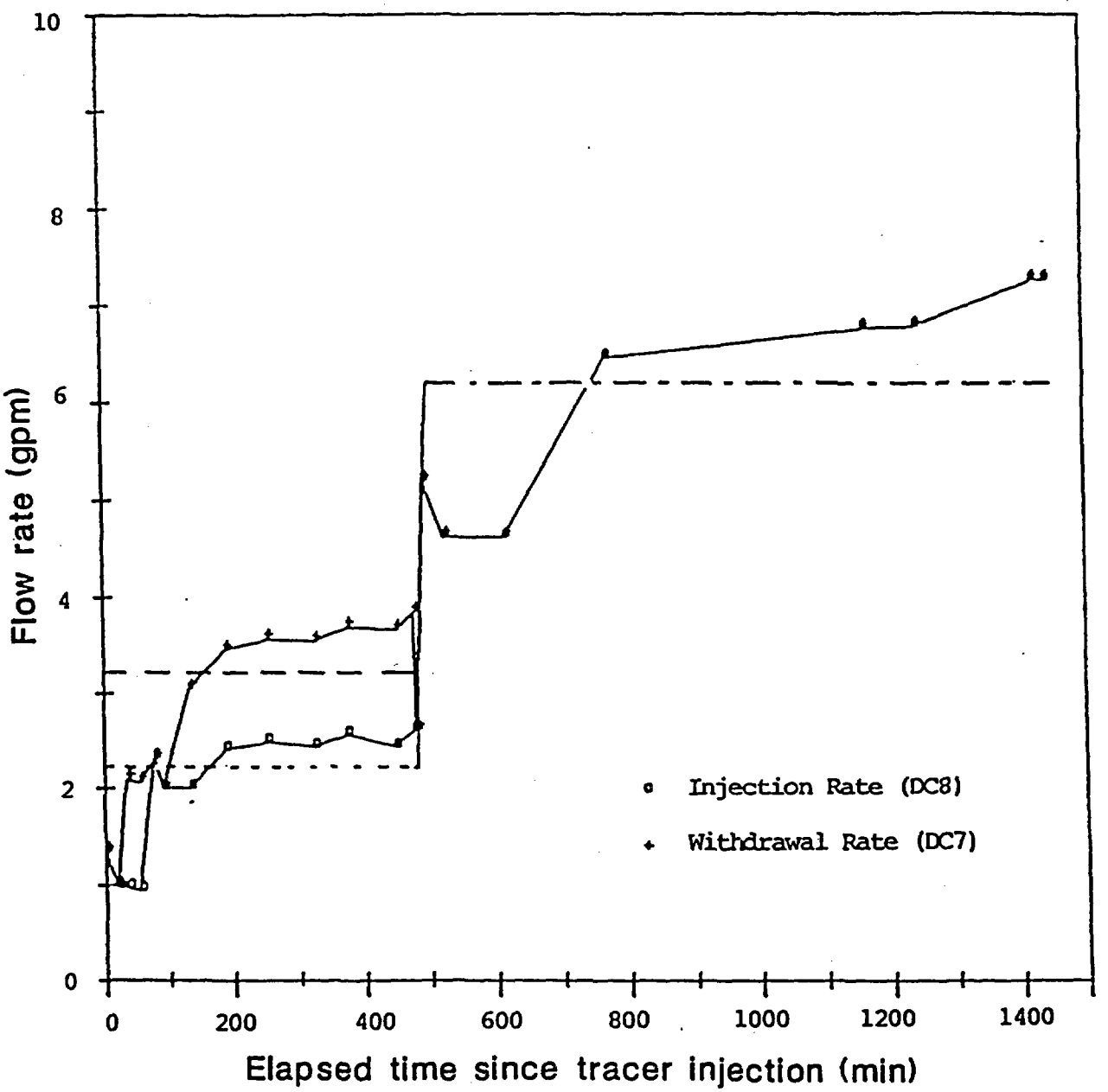

Figure 4.7. Plot of reported pumping and injection rates for Hanford Test 1, with averages assumed for initial numerical modeling.

rate, 2.3, and the average pumping rate, 3.3 gpm) for the first 500 minutes. After that, the flow rate was assumed to increase to about 6.2 gpm.

Using the full composite model, the best fit to the field data is shown in Figure 4.8. Although the simulation matches the first peak closely, the match is not as close for the second and subsequent peaks (compared to Test 2 results). The parameters associated with the simulation results on Figure 4.8 are:

Effective porosity, n_e = 3.2×10^{-4}

Longitudinal dispersivity:

- Formation, α_L = 0.8 ft
- Injection pipe, α_{Lpi} = 2 ft
- Withdrawal pipe, α_{Lpw} = 2 ft

The only way we could find to force a better fit was to vary the pumping rates farther from the reported rates. The pumping rates used in the model for the best-fit simulation on Figure 4.8 are illustrated in Figure 4.9. It is apparent, then, that the accuracy and/or completeness of the reported pumping rates may be questionable for Test 1. As pointed out for Test 2, small errors in the reported pumping rates can cause large errors in simulated peak arrival times and calculated effective porosities.

It is interesting to note that comparable formation dispersivities of 0.8 ft were obtained from the simulations for both Tests 1 and 2. Unlike effective porosity, dispersivity

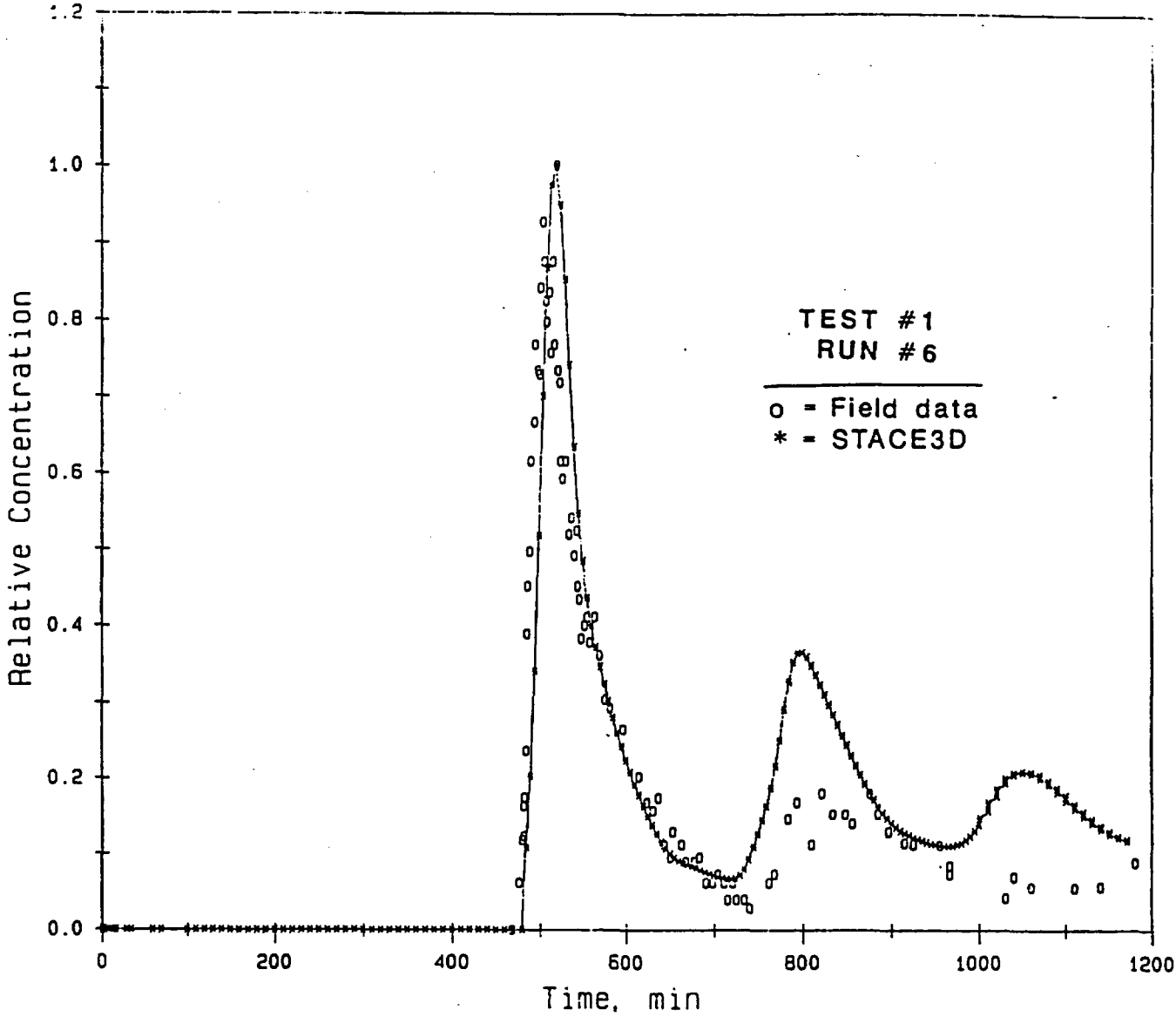

Figure 4.8. Comparison of best-fit simulation to field data using composite STACE3D model for Hanford Test 1.

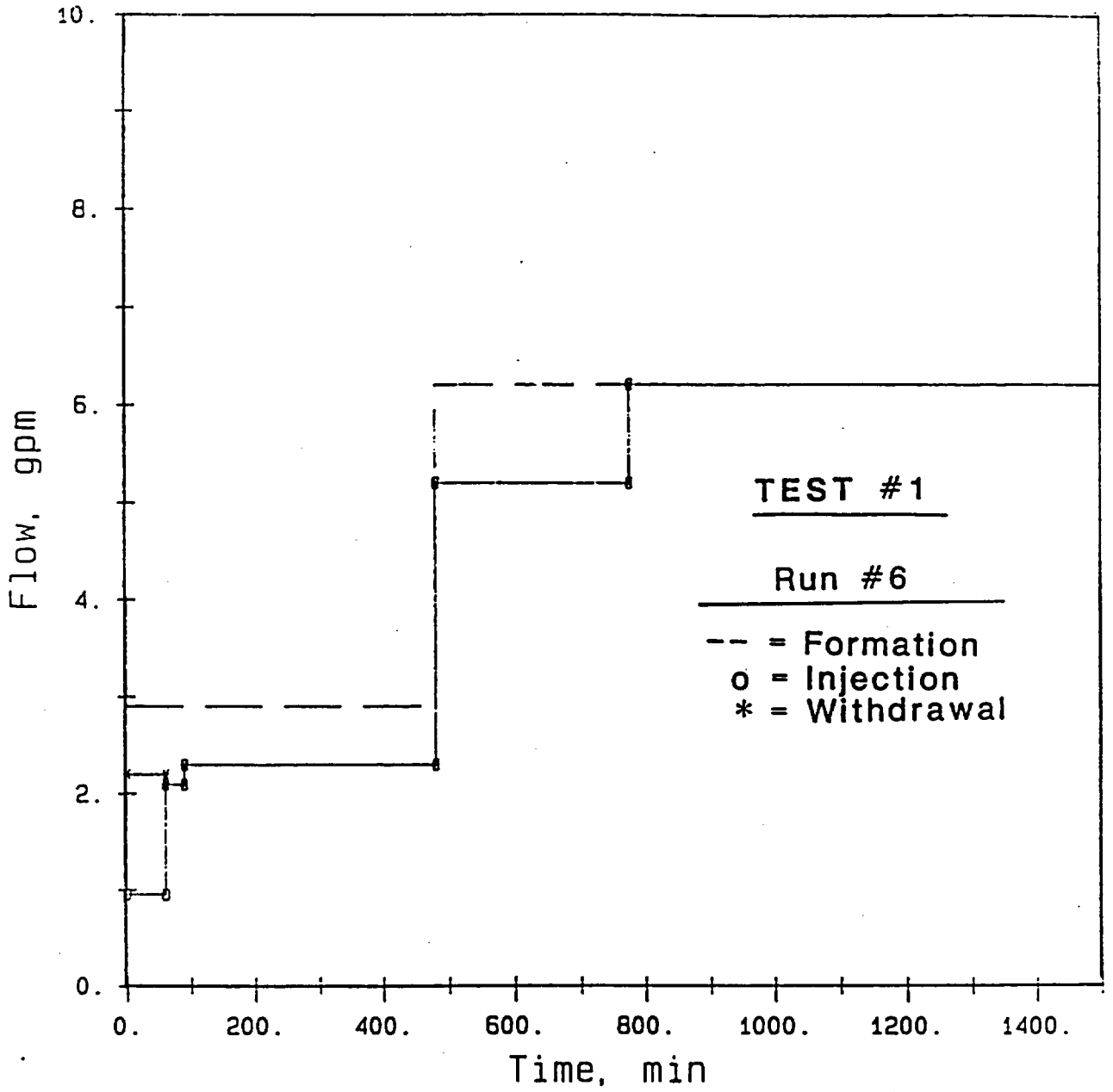

Figure 4.9. Plot of pumping rates used in best-fit simulation for Test 1, using composite STACE3D model.

(α_L) is relatively insensitive to small errors in tracer travel time.

Other analyses were also conducted on the first arrival peak of Test 1 using the basic STACE3D code without pipe-flow components. Figure 4.10 represents a comparison among the STACE3D solution, the Gelhar analytical model solution, and the field data using the porosity and dispersivity parameters determined by Gelhar (1982) using his model. The STACE3D and Gelhar model results agree reasonably well (as they should, when solving the same problem) but neither matches the field data as accurately as might be desired. Porosity and dispersivity were then varied in the basic STACE3D model (without pipe-flow component) to force a closer fit, shown in Figure 4.11, in which longitudinal dispersivity is 1.5 ft and effective porosity is 2.9×10^{-4}. The dispersivity is higher in this case than for the composite model because Taylor's dispersion in the piping is not accounted for in the Figure 4.11 simulations. Also apparent in Figure 4.11 is the absence of the second peak in the simulation, because recirculation could not be properly included without the pipe-flow components of the model.

4.4 Comparative Summary of Tracer Test Analyses

Tracer Test 1 was analyzed by three different analysts using several different approaches:

- SAI, Inc. (Gelhar, 1982) using Gelhar's analytical model

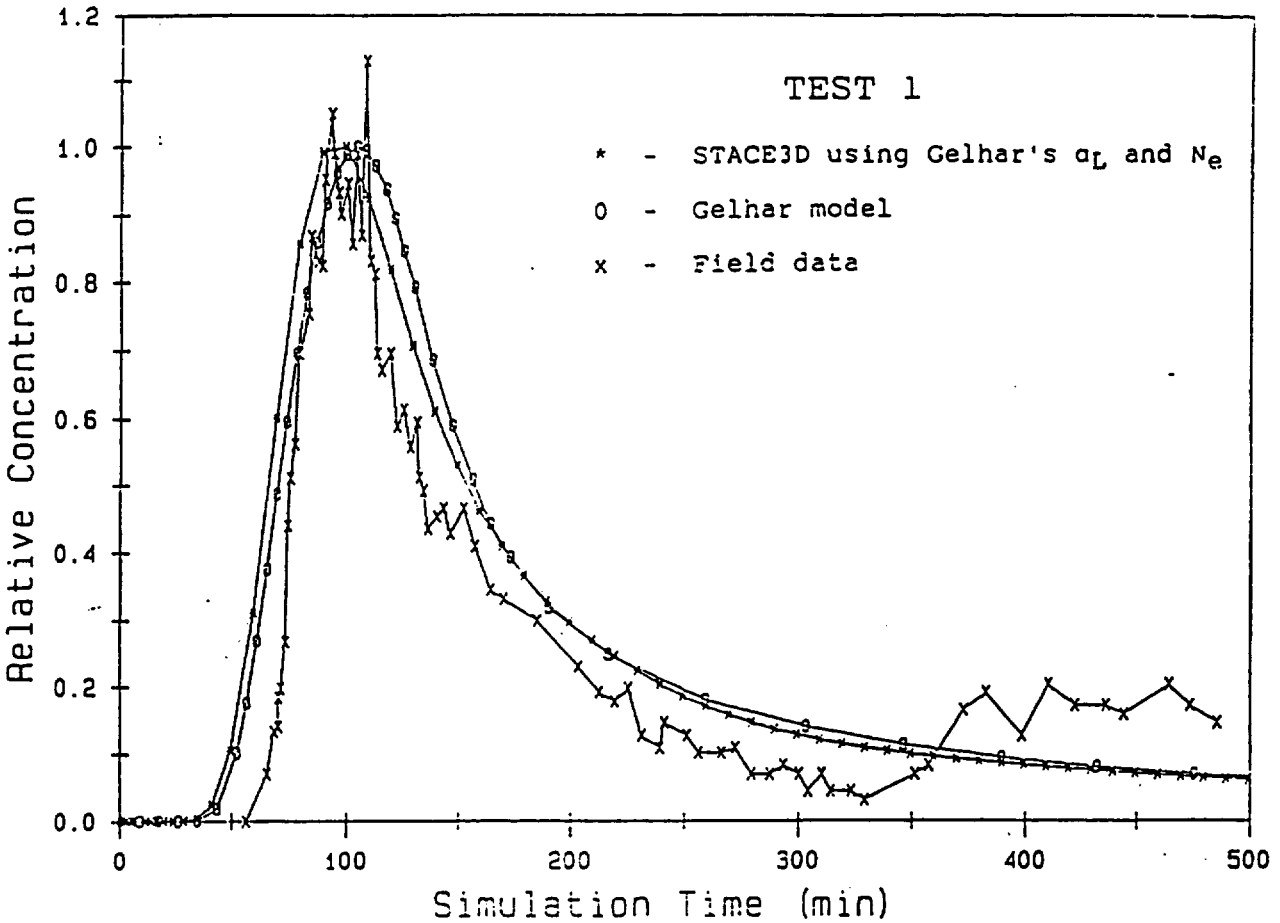

Figure 4.10. Comparison of STACE3D (without pipe-flow component) and Gelhar analytical model simulation with field data for Hanford Test 1, using values of α_L and n_e reported by Gelhar (1982).

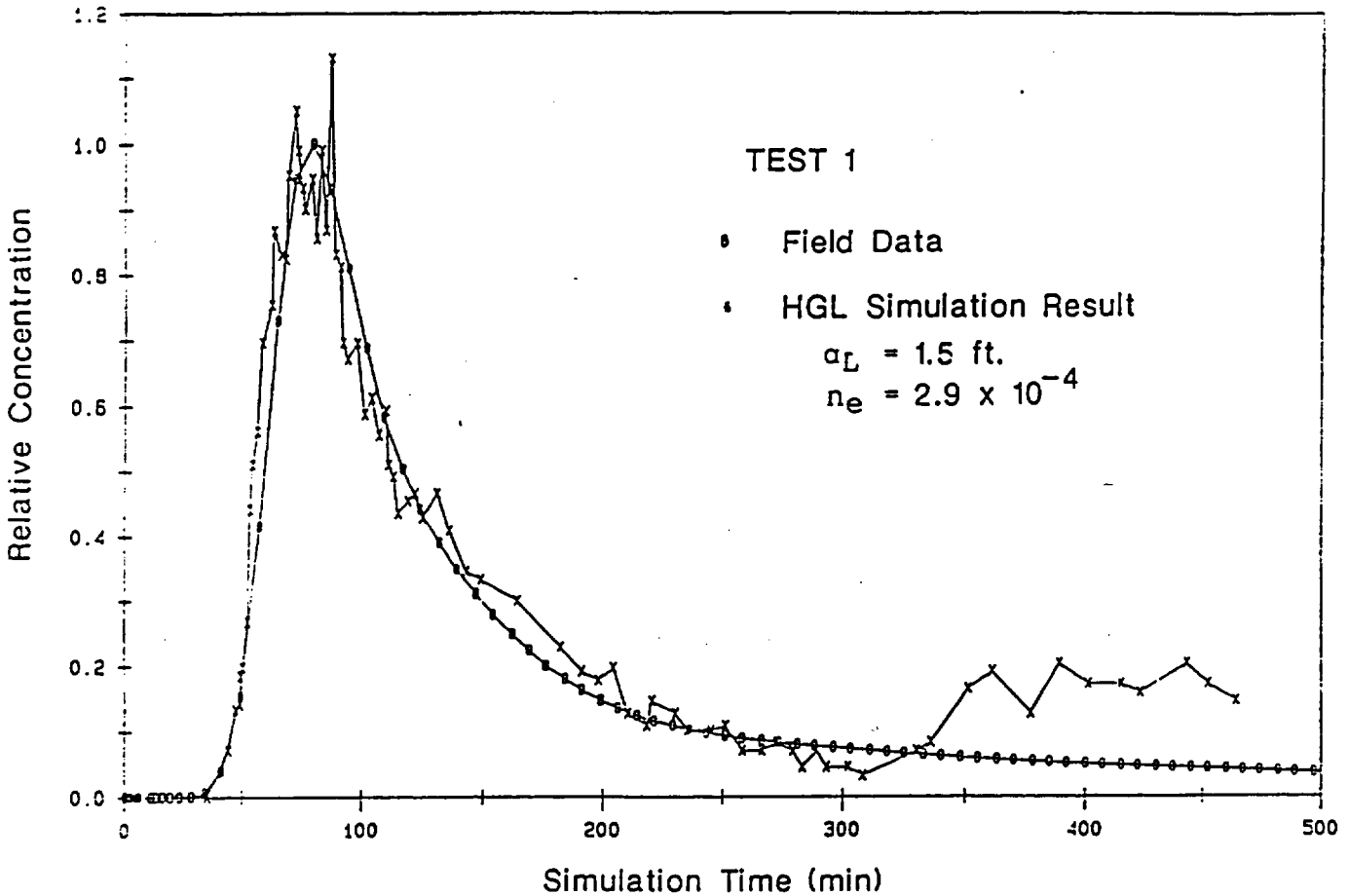

Figure 4.11. Best-fit STACE3D simulation (without pipe-flow component or recirculation) for Hanford Test 1.

- Gelhar (1982) using his analytical model
- HydroGeoLogic, Inc., using basic STACE3D numerical code and composite STACE3D including pipe-flow components.

Test 2 was analyzed by Leonhart and others (1982) of Rockwell Hanford, Inc. using Gelhar's method and by HydroGeoLogic, Inc. using STACE3D numerical code, with and without pipe flow components.

The results of these various analyses are summarized in Table 4.1.

The differences among the results are attributable to several possible factors. Under ideal conditions, each method and each test should yield similar values for effective porosity. The differences in porosity results are apparently due primarily to differences in accounting for the travel time of the tracer in the piping. It is rather surprising, and perhaps fortuitous, that the differences are not greater than indicated. Apparent dispersivities should be dependent on the method used because each method has a different degree of mathematical or numerical dispersion and most of the methods, except for the composite STACE3D model, cannot separate the effects of Taylor's dispersion in the piping from formation dispersion. Therefore, it is not surprising that different methods resulted in different dispersivities, although all results are within the same order of magnitude.

Apparent formation longitudinal dispersivity should be the same for different tests on the same well set, if the same

Table 4.1. Comparison of Parameter Values Obtained from Various Two-Well Tracer Test Analyses.

ANALYSTS	TEST #1		TEST #2	
	α_L (ft)	EFFECT. POR.	α_L (ft)	EFFECT. POR.
HydroGeoLogic				
Using formation model with Gelhar's $T_{up}+T_{down}$	1.5	4.2×10^{-4}		
Using formation model with our $T_{up}+T_{down}$	1.5	2.9×10^{-4}	1.5	1.5×10^{-4}
Using composite pipe-formation model	0.8	3.2×10^{-4}	0.8	1.0×10^{-4}
Gelhar#1/Rockwell#2	1.96	2.1×10^{-4}	2.76	1.2×10^{-4}
SAI	0.78	4.3×10^{-4}	N.A.	N.A.

method of analysis is applied to each test. Both versions of STACE3D (basic formation-only and composite pipe-flow versions) were applied to both Tests 1 and 2. For each version the same formation dispersivity value was obtained: 1.5 ft, using the basic formation version and 0.8 ft using the composite pipe-flow version. This supports the hypothesis that dispersivity should be the same for both tests, but not necessarily the same for both methods.

CONCLUSIONS

The following significant conclusions are derived from this study:

1. The composite STACE3D tracer simulations accurately account for tracer advection and dispersion in the formation as well as in the well-bore conduits, including temporal variations in flow rates and tracer recirculation. This is the first time such a complete and rigorous analysis has been made.

2. The present analysis provides accurate predictions of the times of occurrence for the first and subsequent peaks of tracer concentration at the observation point in the Hanford two-well tracer tests.

3. For test two, which had better flow rate control, the magnitudes and shapes of the first and second simulated peaks closely agreed with field data.

4. For test one, good agreement was obtained between the field data and simulation results until the arrival of the second peak. The discrepancies after the passage of the first peak are probably due, at least in part, to uncertainties in flow rates.

5. Travel time in wells and piping has critical impact on analysis of breakthrough curves for deep-well tracer tests, such as those run at Hanford.

6. Accurate measurement of flow rates and volumes of well bores is critical in determining accurate values of dispersivity and effective porosity and should there-

fore be a prime consideration in designing and planning a deep-well test.

7. The second and subsequent peaks are the result of tracer recirculation and their times of occurrence are controlled primarily by travel time in the well bores for deep-well tests.

8. Taylor's dispersion in well-bore conduits can have significant effects on observed breakthrough curves for tests conducted in deep formations, under laminar flow conditions.

9. For the Hanford Test 2, in which laminar flow apparently prevailed, actual pipe dispersivity values appear to be about one order of magnitude lower than that predicted by Taylor's formulation. This may be caused by roughness in the pipes and other factors which cause flow to deviate from Taylor's assumption of idealized fully developed laminar conditions.

10. Effects of matrix diffusion are probably insignificant for the two tests analyzed but might be significant in a larger scale, longer term test.

11. The two tests analyzed were not designed and conducted in a manner which would reflect effects of matrix diffusion.

12. Longer term and/or larger scale tests are necessary to detect matrix diffusion and to evaluate its controlling parameters.

13. The shape of the tracer breakthrough curves for both tests suggests that the basalt flow top which was tested behaves hydraulically as an isotropic porous medium over the scale of the tests; flow between the wells does not appear to follow preferentially oriented discrete fractures or channels.

REFERENCES

Chatwin, P.C., 1970. The approach to normality of the concentration distribution of a solute in a solvent flowing along a straight pipe, J. Fluid Mech., v. 43, part 2, pp. 321-352.

Dullien, F.A., 1979. Porous Media Fluid Transport and Pore Structure, Academic Press, New York.

Freeze, R.W., and J.A. Cherry, 1979. Groundwater, Prentice-Hall, Inc., Englewood Cliffs, New Jersey.

Gelhar, L.W., 1982. Analysis of two-well tracer tests with a pulse input, Rockwell International Report RHO-BW-CR-131P, prepared for U.S. Department of Energy, 15 p. plus appendices.

Grove, D.B., and W.A. Beetem, 1971. Porosity and dispersion constant calculations for a fractured carbonate aquifer using the two-well tracer method, Water Resour. Res., v. 7, no. 1, pp. 128-134.

Hoopes, J.A., and D.R.F. Harleman, 1967a. Waste water recharge and dispersion in porous media, J. Hydraulics Div. Am. Soc. Civ. Eng., v. 93, pp. 51-71.

Huyakorn, P.S., T.D. Wadsworth, H.O. White, and J.E. Buckley, 1987. STACE3D: A model for seepage and transport analysis using curvilinear elements in three dimensions, Code Documentation Report, prepared for EWA, Inc., 225 p.

Huyakorn, P.S., P.F. Andersen, O. Guven, and F.J. Molz, 1986a. A curvilinear finite element model for simulating two-well tracer tests and transport in stratified aquifers, Water Resour. Res., v. 22, pp. 663-678.

Huyakorn, P.S., P.F. Andersen, F.J. Molz, O. Guven, and J.G. Melville, 1986b. Simulations of two-well tracer tests in stratified aquifers at the Chalk River and Mobile Sites, Water Resour. Res., v. 22, no. 5, pp. 663-678.

Huyakorn, P.S., and G.F. Pinder, 1983. Computational Methods in Subsurface Flow, Academic Press, New York, 473 pp.

Lenda, A., and A. Zuber, 1970. Tracer dispersion in groundwater experiments, Isotope Hydrology, Int. At. Energy Agency, Vienna, Austria, pp. 619-637.

Leonhart, L.S., R.L. Jackson, D.L. Graham, G.M. Thompson, and L.W. Gelhar, 1982. Ground water flow and transport characteristics of flood plain basalts as determined from tracer experiments, Rockwell International Report RHO-BW-5A-220P, prepared for U.S. Dept. of Energy, 13 p.

Nunge, R.J., and W.N. Gill, 1970. Flow through porous media, American Chemical Society, Washington, DC, pp. 179-195.

Taylor, J., 1953. Dispersion of soluble matter in solvent flowing slowly through a tube, Proc. Roy. Soc. A., v. 219, pp. 186-203.

Webster, D.S., J.F. Procter, and I.W. Marine, 1970. Two-well tracer test in fractured crystalline rock, U.S. Geol. Survey Water Supply Paper 1544-I, 22 pp.

Zuber, A., 1974. Theoretical possibilities of the two-well pulse method, Isotope Techniques in Groundwater Hydrology, v. 2, Int. At. Energy Agency, Vienna, Austria, pp. 277-293.